Synthesis of novel heterogeneous photocatalysts based on Rose Bengal for effective wastewater disinfection and decontamination

Alberto Blázquez-Moraleja [a,b], Pilar Moya [c], M. Luisa Marin [b,*], Francisco Bosca [b,*]

[a] Universidad Complutense de Madrid (UCM), Ciudad Universitaria s/n, 28040, Madrid, Spain
[b] Instituto de Tecnología Química (UPV-CSIC), Universitat Politècnica de València-Consejo Superior de Investigaciones Científicas, Avda. de los Naranjos s/n, València 46022, Spain
[c] Instituto Agroforestal del Mediterráneo (IAM-UPV), Universitat Politècnica de València, Avda. de los Naranjos s/n, València 46022, Spain

ABSTRACT

Anionic photosensitizers such as rose Bengal (RB) exhibit low efficiency in the photoinactivation of Gram-negative bacteria. Different strategies have been developed to improve their efficiency being the most effective the addition of the photosensitizer to organic cationic materials. In this context, we have designed the synthesis of a novel heterogeneous photocatalyst based on silica in which the oxidizing properties of singlet oxygen photogenerated by RB have been combined with the chemoattraction of the bacteria to the cationic chains and their biocidal action. Thus, RB and cationic chains have been covalently linked to glass wool to obtain a photocatalyst that showed a highly efficient photodynamic activity against the Gram-positive (*Enterococcus faecalis*) and Gram-negative (*Escherichia coli*) bacteria. In addition, the new heterogeneous photocatalyst also resulted to be efficient in the decontamination of drugs such as diclofenac under visible light irradiation.

1. Introduction

The overuse of antibiotics for the treatment of infectious diseases is the main cause of the development of antibiotic resistance by clinical pathogens. Numerous studies have shown that pharmaceutical compounds are continuously emitted into the environment as a result of anthropological activities. The main drugs found in wastewater are antibiotics, analgesic and anti-inflammatory, disinfectants, etc. These compounds are excreted mainly in the urine (55–80%), less in the faeces (4–30%), as unmetabolized, metabolized or conjugated substances with inactivating bio-substances, which in the case of antibiotics implies a great risk to human health [1–3]. *Escherichia coli* is one of the bacteria that causes the greatest number of infections in mammals and the appearance of multidrug-resistant *E. coli* strains has resulted in significant morbidity and mortality in humans [4,5]. The microbial resistance against conventional methods has directed scientific efforts in the search for alternative and efficient methods of inactivation of microorganisms. In this regard, antimicrobial photoinactivation (PDI) has proven to be a promising method for efficient inactivation against a wide variety of pathogens, including multi-resistant bacteria [6,7]. This method is based on damage to bacteria, viruses, protozoa and fungi by reactive oxygen species (ROS) generated by the activation of a photosensitizer

(PS) by an appropriate light wavelength in the presence of molecular oxygen [8]. It is known that the photoinactivation of Gram-positive and Gram-negative bacteria is dependent on the chemical structure of the PS [9]. In general, neutral, cationic, or anionic PS can easily inactivate Gram-positive bacteria; however, this factor is crucial for Gram-negative bacteria, because only cationic PS have been shown to be efficient in the photoinactivation [10–12]. In addition, there is no relationship between the singlet oxygen quantum yield associated to the PS and the efficiency of Gram-negative inactivation [7]. The difference in the photo-inactivation of the two bacteria is associated with a more complex cell wall in the case of Gram-negative bacteria, which also possess an additional highly organized outer membrane composed of strongly negatively charged lipopolysaccharides, phospholipids, lipoproteins, and proteins [13]. The repulsion forces between the negative charges on the surface of the outer membrane of Gram-negative bacteria and anionic PSs are responsible for the observed inefficiency. Rose Bengal (RB) is one of the anionic PSs with the highest singlet oxygen quantum yield, which as expected, exhibits low efficiency in photoinactivation of Gram-negative bacteria [14]. In this sense, strategies are being developed to favour the electrostatic interaction of the PS with the outer membrane, such as including cationic substituents, or co-administration of a disrupting agents enhancing the penetration of PS to inner cell

---

compartments (eg. L-lysine, ethylenimine, polimyxins, EDTA, etc) [6,10, 15–18]. Their efficiency depends on the number and nature of cationic groups incorporated in the photosensitizer [19,20], which requires complex synthetic protocols and may negatively affect their photo-physical and physicochemical properties [15,21]. Although numerous heterogeneous photocatalysts have been synthesized with RB covalently and electrostatically on various supports: polymeric matrices [22–26], silica matrices [27–29], and fabrics [30–34]; there are only studies showing increased bactericidal action against Gram-negative bacteria using ion exchange resins as cationic polystyrene supports [35,36].

In this context, we propose herein the development of a novel heterogeneous photocatalyst, with the aim to improve the bactericidal action of RB against Gram-negative bacteria, without altering its photophysical properties and its efficacy against Gram-positive bacteria. To achieve this goal, a reference anionic PS, such as RB, and cationic chains are covalently anchored to silica materials such as glass wool (GW). In parallel, RB is covalently attached to GW following an already described protocol giving rise to a second photocatalyst. Comparison of the performance of two photocatalysts in water disinfection and decontamination, illustrates the synergetic effect of the PS and cationic chains.

2. Material and methods

2.1. Synthesis of heterogeneous photocatalysts

GW surface activation was performed by adapting a described procedure [37]. The GW was soaked for 14 h in a 6 M HCl solution and then recovered by decantation, washed ten times with Milli-Q water and then treated with 1 M NH$_3$ for 5 min. Afterwards, the GW was washed again with Milli-Q (3 × 15 min) until pH ~10. The resulting material was washed with EtOH and dried in the oven at 100 °C overnight prior to further functionalization.

2.2. Synthesis of RB-APTES

Rose bengal disodium salt (200 mg, 0.196 mmol) was dissolved in 5 mL of acidic water (pH ~2) for 5 min at room temperature, in order to obtain the protonated acid form. The acid RB was precipitated, recovered via vacuum filtration and dried overnight to get a dark red solid (180 mg, 95%). An excess of SOCl$_2$ (2.0 mL, 27.4 mmol) was added to a stirred solution of acid RB (180 mg, 0.185 mmol) in anhydrous CH$_2$Cl$_2$ (20 mL) under nitrogen atmosphere. The reaction mixture was heated at 40 °C for 15 h under stirring, then the excess of SOCl$_2$ and the solvent were removed at reduced pressure, and the crude product used in the next step without further purification. 3-Aminopropyltriethoxysilane (52 μL, 0.221 mmol) was added into a stirring solution of the previous crude dissolved in anhydrous CH$_2$Cl$_2$ (10 mL) under nitrogen atmosphere. The stirred reaction mixture was heated at 40 °C for 24 h, and then concentrated to give a pink solid (RB-APTES), that was used immediately in the next step without further purification.

2.3. Synthesis of QA-APTES

To a stirred solution of 3-aminopropyltriethoxysilane (635 μL, 2.71 mmol) in dry EtOH (10 mL) was added glycidyltrimethylammonium chloride (808 μL, 5.42 mmol) at room temperature. The stirred reaction mixture was heated for 24 h at 60 °C, under nitrogen atmosphere. The resulting solution was concentrated to give a colourless oil (QA-APTES) that was used immediately in the next step without further purification.

2.4. Synthesis of GW-RB+

Activated GW (12.6 g) was added to a stirred solution of RB-APTES (150 mg, 0.127 mmol) and QA-APTES (500 mg, 0.955 mmol) in dry toluene (250 mL), and the mixture was heated at 110 °C under stirring

for 72 h. After cooling down to room temperature, the material was subsequently washed with toluene (3 ×250 mL), EtOH (3 ×250 mL) and water (3 ×250 mL). Finally, the resulting heterogeneous photocatalyst (GW-RB+) was dried in the oven at 100 °C overnight.

2.5. Synthesis of GW-RB

Activated GW (10 g) was added to a stirred solution of RB-APTES (120 mg, 0.102 mmol) in dry toluene (250 mL), and the mixture was heated at 110 °C for 38 h. After cooling down to room temperature, the material was subsequently washed with toluene (3 ×250 mL), EtOH (3 ×250 mL) and water (3 ×250 mL). Finally, the resulting heterogeneous photocatalyst (GW-RB) was dried in the oven at 100 °C overnight.

2.6. Antibacterial Tests

2.6.1. Photodynamic antibacterial tests

The concentration of the bacterial suspensions was estimated using a Neubauer chamber and adjusted to 1×10^6 bacteria/mL by diluting with sterile distilled water. In all cases, the estimated concentration was further confirmed by a colony count in PCA.

Antimicrobial activity of the materials along the treatments was determined by using standard plate count methods in order to estimate the number of viable bacteria.

In order to ensure the same concentration of photosensitizer, different quantities of synthetized materials were assayed. Hence, GW-RB+ (250 mg) and GW-RB (190 mg) were added to Pyrex glass vials (2.9 cm diameter × 6.5 cm height) containing 20 mL of bacterial suspension (1×10^6 bacteria/mL). Vials were placed in the bottom of the photoreactor (see SI) where irradiance was determined to be 6.75 mW/cm^2. According to this datum, samples were irradiated with a light dose up to a maximum of 48.6 J/cm^2, in the case of *E. coli* (irradiation time = 120 min) and 12.2 J/cm^2 for *E. faecalis* (irradiation time = 30 min). The samples were maintained at constant shaking during the treatments.

Periodically, aliquots (0.5 mL) of the bacterial suspensions were withdrawn from which serial decimal dilutions were made. The appropriated dilutions (100 μL) were then spread plated on PCA plates and incubated overnight to estimate the number of viable bacteria. All the information about data analysis is described in SI.
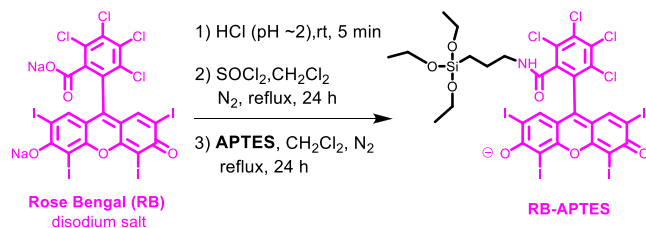
2.6.2. Photodegradation of drugs

GW-RB+ (140 mg), GW-RB (105 mg) and RB aqueous solution (1.59 μM) were added to Pyrex glass tubes containing 10 mL of an aqueous solution of diclofenac (5×10^{-5} M) and irradiated under magnetic stirring. To monitor the removal of the pollutant, aliquots of 180 μL were taken at different irradiation times, and analyzed by HPLC, using 4-nitrobenzoic acid (20 μL of a 0.1 mM solution) as internal standard.
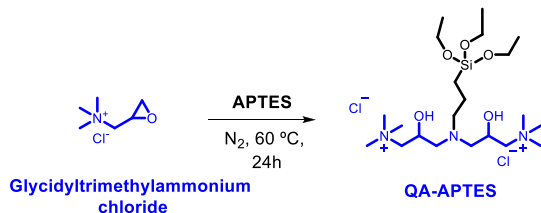
3. Results and discussion

3.1. Synthesis and characterization of novel GW-RB+ and GW-RB photocatalysts

We describe in this work the preparation of the novel heterogeneous photocatalysts (GW-RB+) by covalent anchoring of Rose Bengal and cationic chains, to the inorganic support (GW), as detailed in Scheme 1. For this purpose, RB and the cationic chains were previously functionalized with an aminosilane connector (APTES), in order to control the derivatization of the GW, and thus avoid non-reacting areas due to steric hindrance, low reactivity or accessibility of the amino groups, if the GW surface had been derivatized with APTES, which is the most common strategy [29,37]. In the synthetic protocol developed herein, the acid halide of RB was generated by treatment with thionyl chloride, followed by formation of an amide bond with the amino group of APTES (RB-APTES). In parallel, the amino group of APTES efficiently attacked two equivalents of the epoxy group of glycidyltrimethylammonium
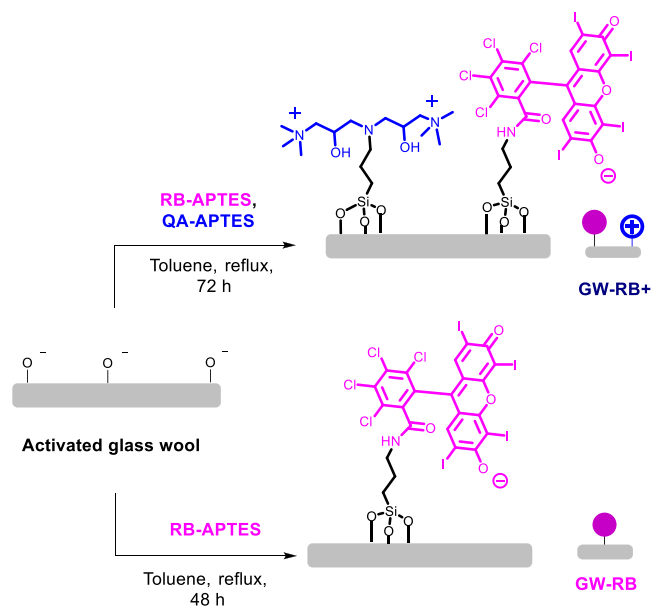
1. Derivatization of RB with APTES to give RB-APTES

Rose Bengal (RB)
disodium salt

1) HCl (pH ~2),rt, 5 min
2) SOCl₂,CH₂Cl₂
   N₂, reflux, 24 h
3) **APTES**, CH₂Cl₂, N₂
   reflux, 24 h

RB-APTES

2. Synthesis of cationic chains (QA-APTES)

**Glycidyltrimethylammonium
chloride**

APTES
N₂, 60 °C,
24h

QA-APTES

3. Covalent anchoring of derivatized RB / cationic chains on GW

**RB-APTES,
QA-APTES**

Toluene, reflux,
72 h

GW-RB+

Activated glass wool

RB-APTES

Toluene, reflux,
48 h

GW-RB

Scheme 1. General procedure for the covalent anchoring of derivatized RB (RB-APTES) / cationic chains (QA-APTES) to GW giving rise to the new photocatalysts: GW-RB+ and GW-RB.

chloride giving rise to the formation of two positive charges per chain (QA-APTES). Next, the covalent immobilization of QA-APTES and RB-APTES to the GW was achieved in a single step. For our dual heterogeneous photocatalyst, GW-RB+, a large excess of the cationic chains versus the PS was employed in an attempt to maximize its efficiency in Gram-negative bacterial inactivation by achieving a high positive charge of the support. With this chemoattraction strategy, unlike homogeneous photocatalysis or the co-administration of disrupting agents, the penetration of the PS inside the cell is not required to trigger the bacterial inactivation mechanism. Although there is a precedent in the literature for covalent anchoring of RB to GW (GW-RB) [29], we decided herein to prepare our GW-RB, from the synthesized RB-APTES, since it will be eventually used for comparative purposes. Moreover, it also demonstrates the versatility of the synthetic process to functionalize the

GW with analogous RB loading. The developed strategy could also be applied to the preparation of future heterogeneous photocatalysts with other PSs.

Microscopic analysis of GW-RB+ (Fig. S1) demonstrated that the covalent anchoring processes of the photosensitizer and cationic chains did not alter the morphology of the fibers. The diffuse reflectance spectra of GW-RB+ and GW-RB showed absorption profiles that resemble the absorption spectra of RB in solution, confirming that in both cases RB is anchored to GW (Fig. S2A). Interestingly, in the two photocatalysts the maximum absorption of RB exhibited a bathochromic shift of 24 nm on GW (λ_{max}= 560 nm) compared to the homogeneous aqueous solution (λ_{max}= 546 nm), in agreement to similar effects described previously for a heterogeneous photocatalyst similar to the GW-RB synthesized herein [29]. This bathochromic shift could be attributed to the less polar environment offered by the amide bond compared to the carboxylic acid when RB is free in water (see Fig. S2B) [38].

Analogously, the fluorescence emission spectra of GW-RB+ and GW-RB also showed bathochromic shifts ($\lambda_{max, GW-RB+}$ = 615 nm and $\lambda_{max, GW-RB}$ = 595 nm) compared to the RB in homogeneous aqueous solution (λ_{max} = 567 nm) (see Fig. S3). The bathochromic effect may be due to covalently anchoring of RB to GW, in agreement to similar effects described previously in the literature for a similar GW-RB [29], and for other xanthene dyes attached to heterogeneous materials (cotton fabric, wool/acrylic fabric, cellulose, etc.) [33,39]. Moreover, this bathochromic shift has also been attributed to a difference in energy stabilization patterns resulting from the loss of hydrogen bonds upon carboxylate derivatization [40,41]. Furthermore, the greater redshift in the case of GW-RB+ could be associated to the presence of the cationic chains which restrict the movement of RB in the GW-RB+ , hindering conformational changes between its transition states.

Next, to determine the loading of RB in the photocatalysts, we have developed a protocol based on the use of pressurized steam that does not alter the physical properties of the GW (see details in SI and Fig. S4). Briefly, the concentration of RB released into the aqueous medium in the autoclaving process (110 °C for 15 min under pressure) from GW-RB+ and GW-RB was determined by UV/VIS spectroscopy. The results revealed that there was a percentage of RB of 0.0155% and 0.0206% (w/w) for GW-RB+ and GW-RB, respectively. This novel protocol has the advantage of being much more sensitive and less tedious than those based on the difference between the initial and final dye concentration in the reaction media. In the latter, it is necessary to combine the multiples washes to which these materials are subjected and arrange the final pH, inducing a greater error in the quantification [42]. Fig. S4c shows that after the pressurized steam process the residual GW do not exhibit the typical RB absorption profile, demonstrating the high efficiency of the developed process.

It is interesting to highlight that the presence of QA-APTES together with RB-APTES in the reaction media for the synthesis of GW-RB+ , only results in a small decrease in the loading of RB (0.0155%, w/w) compared to the one achieved in the synthesis of GW-RB (0.0206%, w/w). We believe that the small interference of the QA-APTES, could be due to the repulsion forces and low solubility of the cationic chains in toluene; that would result into a more slowly incorporation on the surface of the GW than RB-APTES.

The generation of $^1O_2$ when illuminating GW-RB+ and GW-RB was evaluated chemically, upon oxidation of 9,10-diphenylanthracene (DPA) to its corresponding endoperoxide (Scheme S1) [43]. Thus, in the presence of the same amount of PS, the disappearance of DPA, monitored by UV/Vis spectroscopy, was faster under homogeneous conditions (< 90 min); nevertheless, it was also efficient for GW-RB+ and GW-RB (Fig. S5). Even more interestingly, this experiment also demonstrated the enhanced stability of RB upon heterogeneization. In fact, in the case of GW-RB+ and GW-RB the pink color remained after 3 h irradiation (see Fig. S6), while it completely faded after 90 min under homogeneous conditions [44].

In addition, recycling experiments performed under conditions similar to those previously described [29], revealed that both heterogeneous photocatalysts (GW-RB+ and GW-RB) kept good efficiencies for 2 catalytic cycles, when tested in photooxidation of DPA to the corresponding endoperoxide (Fig. S7A). Moreover, although their photocatalytic activity was maintained up to six cycles, the efficiency of GW-RB+ was around 30%, while the efficiency of GW-RB was less than 10% after three cycles.

Finally, the absence of leaching was confirmed by the absorption spectra of the corresponding supernatants after the first catalytic cycle (Fig. S7B).

3.2. Bactericidal activity of GW-RB+ and GW-RB photocatalysts

The bactericidal activity of GW-RB+ and GW-RB was evaluated by exposing them to green light in the presence of bacterial suspensions at an initial concentration of approximately 1×10^6 ufc/mL (Fig. 1).

The photocatalysts showed a highly efficient photodynamic activity against our Gram-positive bacterium *E. faecalis* (Fig. 1). After 10 min of irradiation, both materials were able to induce a reduction of viable colonies of more than 1 $\log_{10}$ unit, being slightly more efficient GW-RB than GW-RB+. Ten minutes later, an important difference in activity levels of the materials was observed. Thus, while GW-RB+ reduced the survival approximately 3 $\log_{10}$ (99.9% of bacterial inactivation), GW-RB reached 5 $\log_{10}$ of reduction, which means a bacterial inactivation of 99.999%, two orders of magnitude more than that obtained with GW-RB+. At the end of the experiment (30 min), both materials showed an efficiency that was practically complete in the case of GW-RB+ (99.99993% bacterial inactivation, which is more than a 6 $\log_{10}$ of survival reduction) and fully complete (100% bacterial inactivation) with GW-RB.

According to the above results, GW-RB+ showed, at intermediate times of exposure, an inactivation kinetic slower than that shown by GW-RB. This result could be explained considering that the experiments were carried out with the same quantity of PS, which involves 250 mg of GW-RB+ versus 190 mg of GW-RB. Thereby, as the amount of GW-RB+ is higher, but with lower number of PS per surface unit than that of GW-RB, the photosensitizing activity of GW-RB+ would be slower than that of GW-RB when the bacteria approach the GW surfaces.

The ANOVA results for *E. faecalis* survival revealed significant effects of all main factors. Thus, GW-RB was significantly more efficient inactivating bacteria than GW-RB+ ($F_{1, 63} = 6.14$; $P = 0.0165$). The irradiation factor (light vs darkness) was highly significant ($F_{1, 63} = 147.68$; $P<0.0001$), clearly showing that, in light conditions, bacterial survival

was efficiently reduced. In addition, an important and significant effect of the time factor was found ($F_{3, 63} = 124.03$; $P<0.0001$), this being that bacterial survival was progressively and negatively affected as exposure time increased. In fact, the LSD multiple range test revealed statistically significant differences for each of the levels (0, 10, 20 and 30 min). Lastly, the statistical analysis disclosed that there were significant interaction effects between the type of material and irradiation factors ($F_{1, 63} = 9.61$; $P = 0.0031$) as well as between irradiation and time factors ($F_{3, 63} = 21.40$; $P<0.0001$).

In the case of our Gram-negative bacterium, *E. coli*, only GW-RB+ was effective inactivating the bacteria, while the bactericidal effect of GW-RB was negligible (Fig. 1). In our conditions, 60 min irradiation of GW-RB+ was required in order to obtain a reduction in survival equal to two orders of magnitude. Nevertheless, after 120 min, the level of reduction in survival was greater than 4 $\log_{10}$, which is fairly close to the level required for disinfection (5 $\log_{10}$). This desired level could be achieved by increasing the exposure time, as it can be extrapolated from the bacterial inactivation kinetics of our data, or also by increasing the amount of GW-RB+ or RB loading and/or the cationic chains on the GW.

Escherichia coli survival results obtained for GW-RB+ were analysed using a two-way ANOVA with irradiation (light vs darkness) and time (0, 60 and 120 min) as factors. Both factors showed statistically significant effects revealing that the material enhanced their efficiency when irradiated with green light ($F = 7.33$; $P = 0.0123$) and when the time of exposure to the light increased ($F = 410.82$; $P<0.001$). In addition, in this case, no significant interaction between the factors was disclosed ($F = 0.68$; $P = 0.5169$). With respect to GW-RB, it has been observed that the total lack of positive charges causes a complete loss of activity, showing, in our experimental conditions, the same negligible levels of bacterial inactivation both with light exposure and without it.

The time required for inactivation of Gram-negative bacteria exceeds that required for Gram-positive bacteria, and is associated to the difference in cell wall structure. The cell wall of Gram-positive bacteria consists of a peptidoglycan layer while that of Gram-negative bacteria possesses an additional outer membrane. This second layer would be responsible for reducing the penetration of singlet oxygen into the cytoplasm, thus conferring to Gram-negative bacteria their lesser susceptibility to photodynamically active bactericides [45,46].

Interestingly, all bacterial tests performed in dark conditions using GW-RB+ always showed some reduction of viable colonies, especially for Gram-negative bacteria where after 60 min of incubation is observed a colonies reduction of 90–95% (ca. 1 $\log_{10}$ unit), a level which remained almost unchanged up to the end of the experiment (120 min). Although part of the reductions could be due to the adsorption of
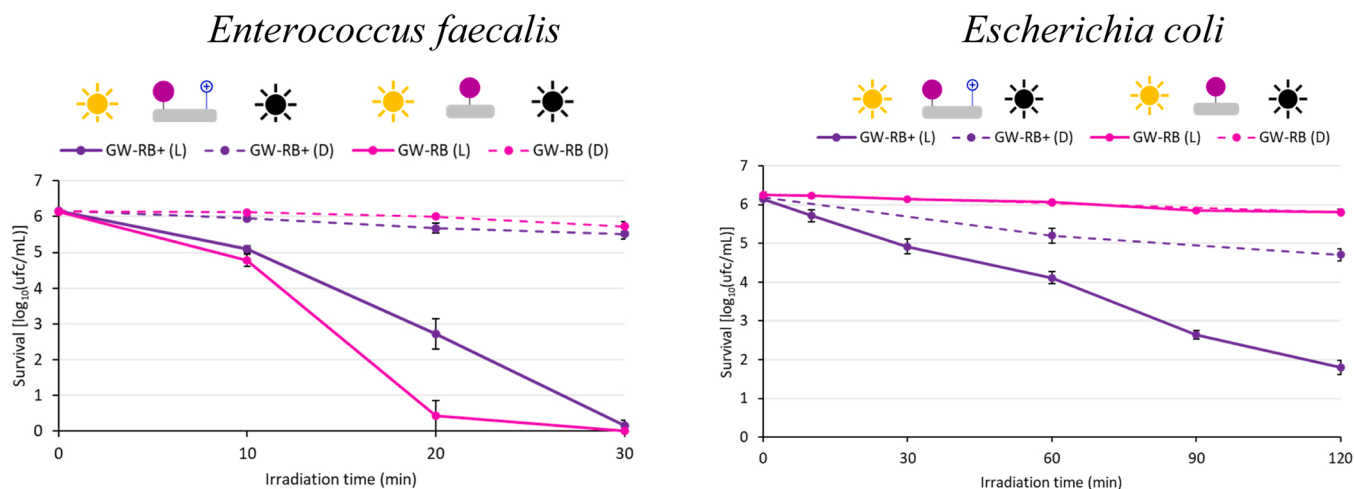

Fig. 1. Photocatalytic antimicrobial activity against Gram-positive (*Enterococcus faecalis*) and Gram-negative (*Escherichia coli*) bacteria under green-light irradiation (8 lamps of λ_{max}=520 nm). Data are means ± standard error (n = 4).

bacteria to GW, this effect is mainly caused by the toxicity of the positive charges of the material, because it is well-known that most bacterial cell walls are negatively charged and the mechanism of the bactericidal action of the polycationic biocides involves destructive interaction with the bacteria wall [47,48].

Therefore, the designed GW-RB+ is able to cause a strong synergistic effect (> 4 $\log_{10}$ to 120 min) between the cationic chains and the action of RB under irradiation which results in a high efficient inactivation of Gram-negative bacteria. Thereby, the cationic charge on surfaces of this heterogeneous organic photocatalyst plays a dual role: its own bactericidal action and to enhance the activity of the photosensitizers which would be mainly produced by the generation of singlet oxygen as an oxidant reactive species. In fact, the formation of $^1O_2$ by GW-RB+ and also by its control photocatalyst GW-RB has been demonstrated (see Fig S5). Thus, the synthetic process developed in this study can be applied for the development of self-disinfecting surfaces in all type of silica-based materials.

### 3.3. Photodegradation properties of GW-RB+ and GW-RB photocatalysts

In order to check the potential of GW-RB+ and GW-RB as photocatalysts for decontamination, we selected the commonly used drug diclofenac (DCF) and evaluated its removal from aqueous media, upon selective excitation of the photocatalysts under green LED light. The anionic charge of DCF would allow evaluating whether the chemoattraction to the cationic chains would favour or not the photodegradation. Thus, the removal of > 90% of DCF was easily achieved in the presence of either GW-RB+ or GW-RB after 3 h irradiation (Fig. 2). However, no differences were observed in the behaviour of the two heterogeneous photocatalysts, indicating that the chemoattraction process between the anionic drug and the positively charged GW-RB+ does not play an important role in the case of small molecules readily soluble in water. In agreement with this hypothesis, no decrease in the concentration of DCF was observed in dark.

Moreover, in the presence of homogeneous RB, removal of DCF followed the same trend as under heterogeneous conditions; however, after 60 min irradiation a plateau was reached, stopping the photodegradation upon 60% removal, mainly due to the much lower photostability of RB compared to the heterogeneous GW-RB+ and GW-RB (see Fig S6).

Although experiments have shown that the two heterogeneous photocatalysts are able to generate singlet oxygen upon irradiation, participation of Type I in the photodegradation of DCF could not be disregarded [49].

4. Conclusions

In this work, we have developed a strategy to covalently anchor an anionic photosensitizer (Rose Bengal, RB) together with cationic chains on a silica-based support such as glass wool (GW), in a single reaction step to obtain a new GW-RB+ photocatalyst. As a result, this novel heterogeneous material showed a high efficiency in the photoinactivation of Gram-positive bacteria, but more interestingly, it also produced the inactivation of the refractive *E. coli* (Gram-negative). It has been demonstrated that this dual design, which includes the cationic chains and RB, causes a synergistic effect that was crucial to produce the photoinactivation of Gram-negative bacteria. In fact, control experiments using GW-RB as a photocatalyst without cationic chains, turned out in photoinactivation of Gram-positive, but it was completely inactive to *E. coli*. Thereby, the cationic charges of heterogeneous organic photocatalyst fulfill two functions, their own bactericidal action and enhance the activity of the photosensitizers which is mainly produced by the generation of singlet oxygen. Moreover, the two heterogeneous photocatalysts were efficient in water decontamination as demonstrated using DCF as a model compound. The synthesis of this kind of dual photocatalysts open the path for efficient antimicrobial
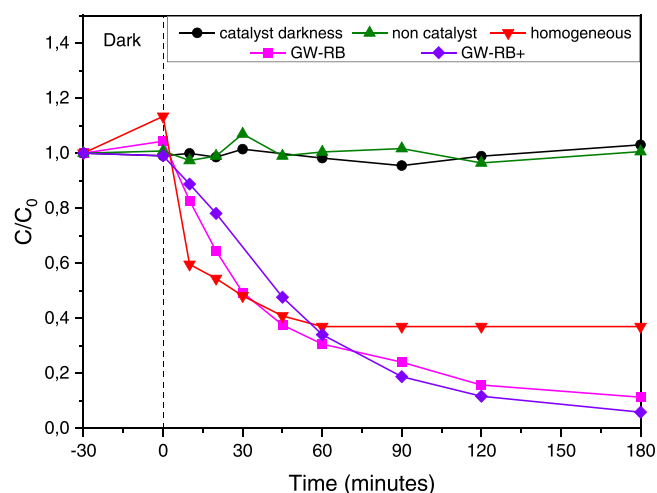
Fig. 2. Degradation of the DCF ($C_0 = 5 \times 10^{-5}$ M) vs time in the presence of GW-RB+ (140 mg), GW-RB (105 mg) and homogeneous RB (1.59 μM) in aerated aqueous solutions (V= 10 mL) and irradiated with green LED light. Catalyst darkness: average of GW-RB and GW-RB+.

photoinactivation (PDI) of multi-resistant pathogens and can be used for the development of self-disinfecting surfaces in all type of silica-based materials.

CRediT authorship contribution statement

Alberto Blazquez-Moraleja: Formal analysis, Investigation, Writing – original draft. **Pilar Moya:** Formal analysis, Writing – original draft. **Francisco Boscá:** Conceptualization, Supervision, Project administration, Writing – review & editing. **M. Luisa Marin:** Conceptualization, Supervision, Writing – review & editing.

Declaration of Competing Interest

The authors declare that they have no known competing financial interests or personal relationships that could have appeared to influence the work reported in this paper.

Data Availability

Data will be made available on request.

Appendix A. Supporting information

Supplementary data associated with this article can be found in the online version at doi:10.1016/j.cattod.2022.11.009.

References

[1] O. Frédéric, P. Yves, Pharmaceuticals in hospital wastewater: Their ecotoxicity and contribution to the environmental hazard of the effluent, Chemosphere 115 (2014) 31–39.

[2] M. Antonopoulou, C. Kosma, T. Albanis, I. Konstantinou, An overview of homogeneous and heterogeneous photocatalysis applications for the removal of

pharmaceutical compounds from real or synthetic hospital wastewaters under lab or pilot scale, Sci. Total Environ. 765 (2021), 144163.

[3] S. Rodriguez-Mozaz, I. Vaz-Moreira, S. Varela Della Giustina, M. Llorca, D. Barceló, S. Schubert, T.U. Berendonk, I. Michael-Kordatou, D. Fatta-Kassinos, J.L. Martinez, C. Elpers, I. Henriques, T. Jaeger, T. Schwartz, E. Paulshus, K. O'Sullivan, K.M. M. Pärnänen, M. Virta, T.T. Do, F. Walsh, C.M. Manaia, Antibiotic residues in final effluents of European wastewater treatment plants and their impact on the aquatic environment, Environ. Int 140 (2020), 105733.

[4] F. Alhashash, V. Weston, M. Diggle, A. McNally, Multidrug-resistant Escherichia coli bacteremia, Emerg. Infect. Dis. 19 (2013) 1699–1701.

[5] L. Falgenhauer, O. Schwengers, J. Schmiedel, C. Baars, O. Lambrecht, S. Heß, T. U. Berendonk, J. Falgenhauer, T. Chakraborty, C. Imirzalioglu, Multidrug-resistant and clinically relevant gram-negative bacteria are present in German surface waters, Front Microbiol 10 (2019).

[6] J. Nakonieczna, K. Wolnikowska, P. Ogonowska, D. Neubauer, A. Bernat, W. Kamysz, Rose Bengal-mediated photoinactivation of multidrug resistant pseudomonas aeruginosa is enhanced in the presence of antimicrobial peptides, Front Microbiol 9 (2018).

[7] N. Kuznetsova, Sensitization of Singlet Oxygen Formation in Aqueous Media, in: T. Nyokong, V. Ahsen (Eds.), Photosensitizers in Medicine, Environment, and Security, Springer Netherlands, Dordrecht, 2012, pp. 267–313.

[8] H. Abrahamse, M.R. Hamblin, New photosensitizers for photodynamic therapy, Biochem. J. 473 (2016) 347–364.

[9] S. George, M.R. Hamblin, A. Kishen, Uptake pathways of anionic and cationic photosensitizers into bacteria, Photochem. Photobiol. Sci. 8 (2009) 788–795.

[10] G. Jori, S.B. Brown, Photosensitized inactivation of microorganisms, Photochem. Photobiol. Sci. 3 (2004) 403–405.

[11] K. Ergaieg, R. Seux, A comparative study of the photoinactivation of bacteria by meso-substituted cationic porphyrin, rose Bengal and methylene blue, Desalination 246 (2009) 353–362.

[12] A. Shrestha, A. Kishen, Polycationic chitosan-conjugated photosensitizer for antibacterial photodynamic Therapy†, Photochem. Photobio. 88 (2012) 577–583.

[13] M.T. Madigan, J.M. Martinko, J. Parker, Brock biology of microorganisms, Pearson Prentice Hall Upper Saddle River, NJ, 2006.

[14] M.C. DeRosa, R.J. Crutchley, Photosensitized singlet oxygen and its applications, 233–234, Coord. Chem. Rev. (2002) 351–371.

[15] S.R.D. Gamelas, A.T.P.C. Gomes, M.A.F. Faustino, A.C. Tomé, J.P.C. Tomé, A. Almeida, L.M.O. Lourenço, Photoinactivation of Escherichia coli with water-soluble ammonium-substituted, Phthalocyanines ACS Appl. Bio Mater. 3 (2020) 4044–4051.

[16] L. Lin, J. Chi, Y. Yan, R. Luo, X. Feng, Y. Zheng, D. Xian, X. Li, G. Quan, D. Liu, C. Wu, C. Lu, X. Pan, Membrane-disruptive peptides/peptidomimetics-based therapeutics: promising systems to combat bacteria and cancer in the drug-resistant era, Acta Pharm. Sin. B 11 (2021) 2609–2644.

[17] V. Pérez-Laguna, Y. Gilaberte, M.I. Millán-Lou, M. Agut, S. Nonell, A. Rezusta, M. R. Hamblin, A combination of photodynamic therapy and antimicrobial compounds to treat skin and mucosal infections: a systematic review, Photochem. Photobiol. Sci. 18 (2019) 1020–1029.

[18] W. Xiang, Z. Xiaoshen, S. Grzegorz, E.-H. Ahmed, H. Ying-Ying, S. Tadeusz, H.M. R. Potassium, Iodide potentiates antimicrobial photodynamic inactivation mediated by Rose Bengal in vitro and in vivo studies, Antimicrob. Agents Chemother. 61 (2017) e00467-17.

[19] M. Merchat, J.D. Spikes, G. Bertoloni, G. Jori, Studies on the mechanism of bacteria photosensitization by meso-substituted cationic porphyrins, J. Photochem. Photobio. B 35 (1996) 149–157.

[20] E. Alves, L. Costa, C.M.B. Carvalho, J.P.C. Tomé, M.A. Faustino, M.G. Neves, A. C. Tomé, J.A.S. Cavaleiro, Â. Cunha, A. Almeida, Charge effect on the photoinactivation of Gram-negative and Gram-positive bacteria by cationic meso-substituted porphyrins, BMC Microbiol 9 (2009) 70.

[21] D.A. Makarov, N.A. Kuznetsova, O.A. Yuzhakova, L.P. Savvina, O.L. Kaliya, E. A. Lukyanets, V.M. Negrimovskii, M.G. Strakhovskaya, Effects of the degree of substitution on the physicochemical properties and photodynamic activity of zinc and aluminum phthalocyanine polycations, Russ. J. Phys. Chem. A 83 (2009) 1044–1050.

[22] D. Valverde, R. Porcar, D. Izquierdo, M.I. Burguete, E. Garcia-Verdugo, S. V. Luis, Rose Bengal immobilized on supported ionic-liquid-like phases: an efficient photocatalyst for batch and flow processes, ChemSusChem 12 (2019) 3996–4004.

[23] V. Fabregat, M.I. Burguete, S.V. Luis, F. Galindo, Improving photocatalytic oxygenation mediated by polymer supported photosensitizers using semiconductor quantum dots as 'light antennas, RSC Adv. 7 (2017) 35154–35158.

[24] X. Yu, Z. Yang, F. Zhang, Z. Liu, P. Yang, H. Zhang, B. Yu, Y. Zhao, Z. Liu, A rose bengal-functionalized porous organic polymer for carboxylative cyclization of propargyl alcohols with CO_2, Chem. Commun. 55 (2019) 12475–12478.

[25] A.M. López-Fernández, I. Muñoz Resta, R. de Llanos, F. Galindo, Photodynamic inactivation of Pseudomonas aeruginosa by PHEMA films loaded with Rose Bengal: potentiation effect of potassium iodide, Polymers 13 (2021).

[26] R.W. Redmond, I.E. Kochevar, Medical applications of Rose Bengal- and riboflavin-photosensitized protein crosslinking, Photochem. Photobio. 95 (2019) 1097–1115.

[27] Y. Gurianov, M. Meistelman, Y. Albo, M. Nisnevitch, F. Nakonechny, Antibacterial activity of Rose Bengal entrapped in organically modified silica matrices, Int. J. Mol. Sci. 23 (2022).

[28] Y. Guo, S. Rogelj, P. Zhang, Rose Bengal-decorated silica nanoparticles as photosensitizers for inactivation of gram-positive bacteria, Nanotechnology 21 (2010) 65102.

[29] R.I. Teixeira, N.C. de Lucas, S.J. Garden, A.E. Lanterna, J.C. Scaiano, Glass wool supported ruthenium complexes: versatile, recyclable heterogeneous photoredox catalysts, Catal. Sci. Technol. 10 (2020) 1273–1280.

[30] Z. Yan, W. Wei, H. Xun, S. Anguo, Rose Bengal immobilized on wool as an efficiently "green" sensitizer for photooxygenation reactions, Chem. Lett. 41 (2012) 1500–1502.

[31] P. Tang, A.Y. El-Moghazy, B. Ji, N. Nitin, G. Sun, Unique "posture" of rose Bengal for fabricating personal protective equipment with enhanced daylight-induced biocidal efficiency, Mater. Adv. 2 (2021) 3569–3578.

[32] F. Jin, S. Liao, Q. Wang, H. Shen, C. Jiang, J. Zhang, Q. Wei, R.A. Ghiladi, Dual-functionalized luminescent/photodynamic composite fabrics: Synergistic antibacterial activity for self-disinfecting textiles, Appl. Surf. Sci. 587 (2022), 152737.

[33] W. Chen, J. Chen, L. Li, X. Wang, Q. Wei, R.A. Ghiladi, Q. Wang, Wool/acrylic blended fabrics as next-generation photodynamic antimicrobial materials, ACS Appl. Mater. Interfaces 11 (2019) 29557–29568.

[34] T. Zhang, H. Yu, J. Li, H. Song, S. Wang, Z. Zhang, S. Chen, Green light–triggered antimicrobial cotton fabric for wastewater disinfection, Materials Today, Physics 15 (2020), 100254.

[35] C.A. del Valle, V. Pérez-Laguna, I.M. Resta, R. Gavara, C. Felip-León, J.F. Miravet, A. Rezusta, F. Galindo, A cost-effective combination of Rose Bengal and off-the-shelf cationic polystyrene for the photodynamic inactivation of Pseudomonas aeruginosa, Mater. Sci. Eng. C Mater. Biol. Appl. 117 (2020), 111302.

[36] R. Gavara, R. de Llanos, V. Pérez-Laguna, C. Arnau del Valle, J.F. Miravet, A. Rezusta, F. Galindo, Broad-spectrum photo-antimicrobial polymers based on cationic polystyrene and Rose Bengal, Front Med (Lausanne) 8 (2021).

[37] A. Elhage, B. Wang, N. Marina, M.L. Marin, M. Cruz, A.E. Lanterna, J.C. Scaiano, Glass wool: a novel support for heterogeneous catalysis, Chem. Sci. 9 (2018) 6844–6852.

[38] A. Torres-Martínez, B. Bedrina, E. Falomir, M.J. Marín, C.A. Angulo-Pachón, F. Galindo, J.F. Miravet, Non-polymeric nanogels as versatile nanocarriers: intracellular transport of the photosensitizers Rose Bengal and hypericin for photodynamic therapy, ACS Appl. Bio Mater. 4 (2021) 3658–3669.

[39] D. Staneva, S. Yordanova, E. Vasileva-Tonkova, S. Stoyanov, I. Grabchev, Photophysical and antibacterial activity of light-activated quaternary eosin Y, Open Chem. 17 (2019) 1244–1251.

[40] P.C. de Souza Pereira, P.F. do, A. Costa, D.S. Pellosi, I.R. Calori, B.H. Vilsinski, B. M. Estevão, N. Hioka, W. Caetano, Photophysical properties and interaction studies of Rose Bengal derivatives with biomimetic systems based in micellar aqueous solutions, J. Mol. Liq. 230 (2017) 674–685.

[41] M.M. Martin, Hydrogen bond effects on radiationless electronic transitions in xanthene dyes, Chem. Phys. Lett. 35 (1975) 105–111.

[42] M. Günay, W.J. Jasper, Limitations in predicting dyebath exhaustion using optical spectroscopy, Color. Technol. 126 (2010) 140–146.

[43] M.I. Burguete, F. Galindo, R. Gavara, S.V. Luis, M. Moreno, P. Thomas, D. A. Russell, Singlet oxygen generation using a porous monolithic polymer supported photosensitizer: potential application to the photodynamic destruction of melanoma cells, Photochem. Photobiol. Sci. 8 (2009) 37–44.

[44] M.P. Serrano, M. Rafti, A.H. Thomas, C.D. Borsarelli, Photosensitizing properties of hollow microcapsules built by multilayer self-assembly of poly(allylamine hydrochloride) modified with rose Bengal, RSC Adv. 9 (2019) 19226–19235.

[45] T.A. Dahl, W.R. Midden, P.E. Hartman, Comparison of killing of gram-negative and gram-positive bacteria by pure singlet oxygen, J. Bacteriol. 171 (1989) 2188–2194.

[46] M.R. Hamblin, T. Hasan, Photodynamic therapy: a new antimicrobial approach to infectious disease? Photochem. Photobiol. Sci. 3 (2004) 436–450.

[47] A. Muñoz-Bonilla, M. Fernández-García, Polymeric materials with antimicrobial activity, Prog. Polym. Sci. 37 (2012) 281–339.

[48] E.-R. Kenawy, S.D. Worley, R. Broughton, The chemistry and applications of antimicrobial polymers: a state-of-the-art review, Biomacromolecules 8 (2007) 1359–1384.

[49] R. Martinez-Haya, M.A. Miranda, M.L. Marin, Type I vs type II photodegradation of pollutants, Catal. Today 313 (2018) 161–166.